

## SODIUM TRANSPORT MODES IN AMTEC ELECTRODES

R. M. Williams, M.L. Homer, L. Lara, R. H. Cortez, J. Miller, B. Jeffries-Nakamura, M. L. Underwood,  
A. Kisor, D. O'Connor, V. B. Shields, K. S. Manatt, M. A. Ryan

Jet Propulsion Laboratory, California Institute of Technology  
4800 Oak Grove Drive, Pasadena, CA 91109  
(818) 354-2727

Roger M Williams@jpl.nasa.gov

### ABSTRACT

Transport of alkali metal atoms through porous cathodes of alkali metal thermal-to-electric converter (AMTEC) cells is responsible for significant, reducible losses in the electrical performance of these cells. Sodium transport has been characterized in a variety of AMTEC electrodes and several different transport modes clearly exist.

Free molecular flow is the dominant transport mechanism in clean porous molybdenum and tungsten electrodes, and contributes to sodium transport in all porous electrodes, including  $WPt_2$ ,  $WRh_3$ , and TiN.

Molybdenum and tungsten electrodes containing phases such as  $Na_2MoO_4$  and  $Na_2WO_4$  exhibit very efficient sodium ion transport through the electrode in the ionic conducting phase. These electrodes also show reversible electrochemical reactions in which sodium ions and electrons are inserted or removed from into phases such as  $Na_2MoO_4$  and  $Na_2Mo_3O_6$  which are present in the electrode

$WPt_2$  and  $WRh_3$  electrodes typically exhibit both free molecular flow transport as well as an enhanced thermally activated transport mode which is probably surface and/or grain boundary diffusion of sodium in the alloy electrode. Data for large area  $WPt_2$  electrodes within a cylindrical heat shield are reported in this paper. Sodium transport away from these electrodes is effected by both the electrode's properties and the exterior environment which inhibits sodium gas flow to the condenser.

Liquid alloy electrodes have been examined and have fairly efficient transport properties by liquid phase diffusion, but have generally not been considered

advantageous for development.

Titanium nitride, TiN, electrodes used in AMTEC cells, and similar electronically conducting refractory compounds such as  $TiB_2$  and  $NbN$  are always physically porous to some degree as formed by sputter deposition or screen printing, and these compounds sinter quite slowly. Hence free molecular flow is always a significant sodium transport mode in these electrodes. However, the sodium transport rate computed from the physical morphology of the electrodes is not as efficient as actual sodium transport in TiN electrodes, implicating an enhanced transport mode, which remains operational at lower AMTEC operating temperatures. Some TiN electrodes also have been found to exhibit electrochemical reactions involving electrode phases which persist in sodium exposure test cells at 1223K, as reported in this paper.

### INTRODUCTION

The alkali metal thermal-to-electric converter (AMTEC) is a high power, high efficiency, electrochemical concentration cell. It uses sodium as the working fluid and a porous metal electrode (PME) on the low pressure side of a beta" alumina solid electrolyte (BASE) ceramic across which a high sodium activity gradient to a liquid sodium or high pressure gaseous sodium reservoir at  $T = 900 - 1300K$ . The activity gradient is controlled by the device's current density in operation, by electrochemical shunt currents and leakage, by the mass transport characteristics of the entire AMTEC cell, and by the condenser temperature. In laboratory test cells with small electrodes and non-optimized cell volume, with condenser  $T < 600K$ , and currents  $\sim 1-2 A/cm^2$ , sodium transport properties of the PME dominate the interfacial BASE/PME sodium

pressure when cell current is not zero. In prototype AMTECs such as those made by Advanced Modular Power Systems, Inc., when the cell is at open circuit the sodium pressure at the PME is dominated by sodium gas produced by electrochemical shunts. There is a significant sodium pressure drop between the PME exterior and the condenser due to cell geometry and heat shields. This pressure drop contributes to the current dependent sodium activity at the PME/BASE interface in the same manner as do the pressure drops within the PME.

Because AMTEC is a high current, low voltage device, all internal losses in the cell must be minimized. This requires a detailed understanding of how mass transport, kinetics, and ohmic resistance affect the cell's current-voltage curve. The fundamental principles of the AMTEC cell were described in a paper by Weber<sup>1</sup>, and an integrated, quantitative model of kinetics and transport in AMTEC cells was later developed.<sup>2,3</sup> Complete resolution of sodium transport processes from charge transfer processes is not possible in real AMTEC electrode phenomena; very efficient mass transport away from sites where the charge transfer process is slow does not help electrode performance, nor does a very efficient charge transfer process occurring at a site without an effective transport mode to the electrode exterior. Complete resolution is possible only if the exchange current and the mass transport limitations are uniform over all microscopic area elements of the electrode. However, we routinely resolve characteristic values of the exchange current ( $B$ ) and mass transport or morphology parameter ( $G$ ), recognizing that these are weighted values of distributed characteristics. Pre-test and post-mortem characterization of electrodes by scanning electron microscopy (SEM) energy dispersive spectroscopy (EDS) and x-ray diffraction (XRD) for morphological and composition evaluation of the electrodes allows us to determine the initial and final properties of the electrodes in comparison with their performance evolution, for development of life models.

Sodium transport through electrodes on the low pressure side of the AMTEC cell may be characterized using electrochemical impedance spectroscopy (EIS) which provide the initial data critical to development of a quantitative model for the mixed kinetics/transport control generally occurring in these electrodes.<sup>2,7</sup> EIS has been an important tool in building a fundamental, experimentally verified model for the processes operating in AMTEC electrodes. It also provides the most thorough characterization of an electrode, although the transport parameters, as well as

the exchange current and ohmic resistance, can also be obtained from some high quality current-voltage curve data. The cell's ohmic resistance is generally treated as a series resistance, without great error, although part of it is in parallel to some electrochemical impedances.

Even high quality current-voltage curves obtained under conditions of high ambient sodium pressure may not allow reliable derivation of  $G$  and  $B$  and the cell's ohmic resistance. In the limit that the  $iV$  curve becomes a straight line, all three of these terms will contribute to the slope and will not be resolved. Impedance data under the same conditions, measured at several cell potentials, will allow separation of the ohmic series resistance from the electrochemical impedance which contributes only at frequencies  $< 10^4$  Hz. The resistive elements of the electrochemical impedance are effectively bypassed by charging of large parallel capacitances and pseudocapacitances at higher frequencies.

Transport mechanisms include free-molecular flow, surface and grain boundary diffusion of sodium, bulk diffusion of sodium atoms through condensed phases, and sodium ion conduction with charge transfer at the cathode exterior surface. Bulk diffusion of sodium through liquid alloy electrodes was first observed by researchers at Ford; these electrodes were high performance electrodes, but because of issues related to fabrication and durability they have not been investigated for prototype cells.<sup>8</sup> Later, liquid lead and tin cathodes were re-examined by Fang and Wendt and were found to have generally very good properties.<sup>9</sup>

Free molecular flow dominates in the dc operation of clean, porous Mo and W electrodes (power density of  $0.5 \text{ W/cm}^2$  at  $T_2 = 1200\text{K}$ ), but surface diffusion plays a more important role in  $\text{WRh}_3$  and  $\text{WPt}_2$  high performance electrodes (power density of  $0.8 \text{ W/cm}^2$  at  $T_2 = 1200\text{K}$ ).<sup>2,3,6,7</sup> The most important distinction between these classes of electrodes was derived from temperature cycling experiments with Mo and  $\text{WRh}_3$  electrodes. Using a free-molecular flow model, the value of  $G$  for these electrodes was determined from impedance data. The Mo electrodes showed little variation in derived values of  $G$  with temperature, and these were in fair agreement with  $G$ 's calculated for a somewhat idealized structure based on the electrode morphology observed by SEM. The  $\text{WRh}_3$  electrodes showed a large, reversible decrease in the  $G$  derived from impedance as temperature increased. These  $\text{WRh}_3$  electrodes show rather low porosity on SEM examination. However, some thin ( $< 1.0 \mu\text{m}$ )

WRh<sub>3</sub> and WPt<sub>2</sub> electrodes may exhibit fairly porous morphology in SEM and little temperature dependence of G derived from impedance.

Electrodes containing molybdenum or tungsten oxides before operation in AMTEC cells initially show excellent transport due to ionic conduction of sodium ions through liquid sodium molybdate or tungstate in the electrode's pores.<sup>4,10,11</sup> Na<sub>2</sub>MoO<sub>4</sub> and Na<sub>2</sub>WO<sub>4</sub> evaporate in tens to hundreds of hours at typical AMTEC operating temperatures. In Na<sub>2</sub>MoO<sub>4</sub>/Mo electrodes the electronically conducting phase Na<sub>2</sub>Mo<sub>3</sub>O<sub>6</sub>, which is a sodium addition compound to MoO<sub>2</sub>, is also stable at lower sodium activities, and can be slowly converted to Mo and Na<sub>2</sub>MoO<sub>4</sub> by addition of more sodium, or to MoO<sub>2</sub> by removal of sodium. These conversions suggest that it is a poor sodium ion conductor. Along with Na<sub>2</sub>MoO<sub>4</sub>, it may be responsible for the very high efficiency of charge transfer as well as sodium transport in these electrodes.<sup>2,4,10,11</sup> Ionic conduction is also effective in Mo/BASE cermet electrodes, but these have not shown high power densities reproducibly.

TiN electrodes, and to a lesser extent related electrodes such as TiC, TiB<sub>2</sub>, NbN and NbC, have been extensively tested for AMTEC applications, but their sodium transport mechanisms remain poorly understood.<sup>12-17</sup> It is known that these electrodes are quite stable, and offer electrochemical performance which seems inconsistent with a sodium transport mechanism depending on free molecular flow. No activation energies associated with sodium transport in these electrodes have been reported.

## EXPERIMENTAL

The electrode test cell (ETC) and the sodium exposure test cell (SETC) used by JPL for characterization of AMTEC electrodes and cells have been described previously.<sup>2-7</sup>

The ETC allows more thorough analysis of the electrical and electrochemical performance of an electrode, compared with an AMTEC cell with a single large area cathode. The ETC has a large number of electrical feedthroughs into the cell for leads and sometimes thermocouples to the external PME's. It has an unrealistically large condenser to BASE tube surface ratio compared with prototype AMTEC cells and is therefore not used for thermal characterization of the overall AMTEC device. Because it can be used with several cathodes operating independently or in parallel,

the ETC may be used to compare the transport limitations for single electrodes vs. groups of electrodes within the same heat shield, allowing separation of electrode transport limitations from limitations due to flow past the heat shield.

The sodium exposure test cell, SETC, is simply an evacuated stainless steel tube with an external furnace for temperature control, which has several insulating electrical feedthroughs, whose insulators extend far enough into the hot zone of the furnace to prevent sodium condensation. Sodium vapor is provided by a pool of sodium at the cool end of the cell, which has provision for independent temperature control using a heating tape, in order to vary the vapor pressure as required. Electrodes deposited on small sections of BASE tube, or on other small ceramic specimens may be mounted on an internal support.

This cell allows long-term exposure tests of electrodes on BASE in sodium vapor with maximum convenience, and also ideally permits as complete characterization of the electrode's electrochemical and electrical properties as is possible in the ETC, but generally requires a symmetrical pair of electrodes.

## RESULTS AND DISCUSSION

Porosity of WRh<sub>3</sub>, WPt<sub>2</sub>, and TiN electrodes as determined by post-mortem analysis of electrode morphology by SEM is not high enough to account for their favorable transport performance via a free-molecular flow mechanism alone, in contrast to the transport performance of Mo and W electrodes.

The value of the dimensionless transport parameter, G, derived from both impedance data and current voltage curves is not determined by a frequency-dependent fit, but rather represents the model dependent transport contribution to the potential-dependent dc resistance, indicated by the length of the impedance arc along the real axis, or the potential dependent slope of the current voltage curve.

More information can be obtained from a frequency dependent fit to the impedance data, such as the interfacial capacitance and the high frequency value of the charge transfer resistance, but in general reduction of the transport process to its components has not been possible. Extraction of the impedance arc due

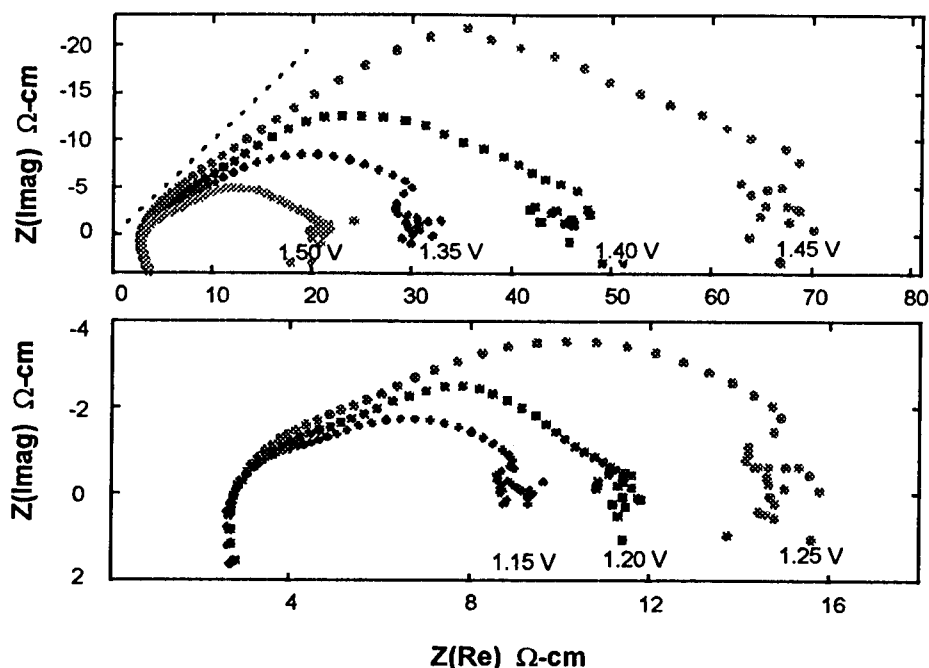


Figure 1: Impedance at several different cell potentials for 56 cm<sup>2</sup> WPt<sub>2</sub> electrode in AMTEC ETC.

to the transport process alone can be accomplished by successive subtraction of the series resistance (and inductance) from the impedance, followed by the sequential subtraction of the parallel interfacial capacitance from the admittances determined after the first step, and then the generalized charge transfer resistance after reversion to impedance data.<sup>3</sup> The resulting data which characterize the overall transport process contain contributions from free-molecular flow transport, surface diffusion, and desorption/ adsorption processes within the pores and at the exterior electrode surface, but cannot be directly fit.

Values of  $G$  for mature Mo, WPt<sub>2</sub>, and WRh<sub>3</sub> electrodes have been obtained for a large number of high performance electrodes at a wide range of operating temperatures in the ETC. Impedance spectra of a large number of Mo electrodes operated at almost all accessible AMTEC conditions yield no clear temperature dependence of the transport parameter. Impedance spectra of thin (0.5  $\mu\text{m}$ ) Mo electrodes gave a transport parameter,  $G$ , of about 50, which is in agreement with calculation with respect to a free molecular flow process for the observed morphology.<sup>2,3,18</sup>

The transport parameter,  $G$ , in some WRh<sub>3</sub> electrodes has shown a strong increase with decreasing temperature in the temperature range of 730 to 1130K.

This phenomenon is observed at sodium vapor pressures of 0.2 to 4.0 Pa, and is measured from electrode limiting current densities of 30 to 1400 A/m<sup>2</sup> in the SETC and from WRh<sub>3</sub> electrodes in the ETC. Some tests showed a limiting value at lower temperatures, indicating that the transport process does eventually become dominated by free molecular flow.  $G$ 's for WRh<sub>3</sub> electrodes at temperatures near 1200K are as low as about 10-15.

WPt<sub>2</sub> electrodes have not shown clear activated performance in ETC tests, and in one ETC test mature WPt<sub>2</sub> electrodes, after 400 hours above 1100K, had nearly temperature independent  $G$ 's from 600 to 900 C, but transport in these electrodes is too efficient to be purely free molecular flow. The best electrode had a  $G$  of about 30, but if the heat shield effect is subtracted the electrode contribution is about 20.

Figure 1 shows impedance spectra as a function of cell potential for four 14.1cm<sup>2</sup> WPt<sub>2</sub> electrodes operated in parallel at an average electrode temperature of about 1130K. The linear slope on the high frequency side of the arcs indicate transport behavior of a finite Warburg impedance, characteristic of a diffusion process through a thin layer. The Warburg impedance does not dominate the electrochemical impedance at the highest frequencies. There the finite Warburg is shorted through its capacitive component but the charge transfer resistance in series with it, is still important. The

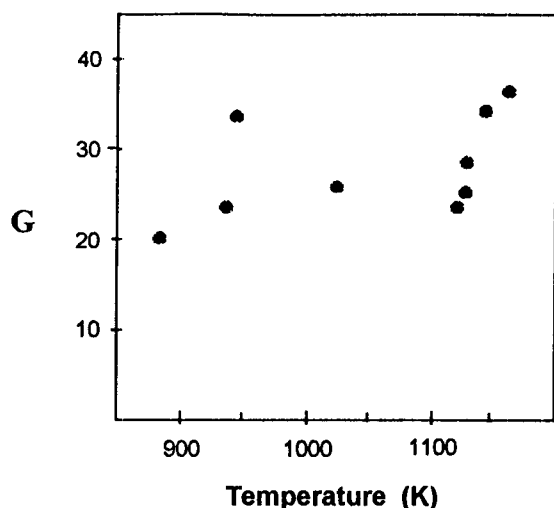


Figure 2: Electrode Morphology Parameter,  $G$ , vs Temperature for one  $14.1 \text{ cm}^2$   $\text{WPt}_2$  electrode after 400 hours.

structure in the impedance arcs near the low frequency intercept is not understood.

Figure 2 shows the value of  $G$ , the transport parameter, derived from impedance spectra taken at several cell temperatures for a  $14.1 \text{ cm}^2$   $\text{WPt}_2$  electrode after about 400 hours of 1150 K operation.

Figure 3 shows the value of the apparent charge transfer resistance,  $R_{\text{ACT}}$ , at 1.45 Volts, for four  $14.1 \text{ cm}^2$   $\text{WPt}_2$  electrodes and combinations of these four electrodes.  $G$ 's for the individual electrodes were 29, 35, 40, and 45 and were about equal to  $R_{\text{ACT}}(1.45\text{V})$  expressed in  $\Omega/\text{cm}^2$ . All of the electrodes had an open circuit voltage,  $E_{\text{oc}} > 1.45$  volts, and their temperatures ranged from 1120K to 1190K. We can not compute a single valued  $G$  for an electrode with a large temperature gradient, so the data are presented in this unbiased fashion. The slope, (resistance change)/(area change), is due primarily to the heat shield, and the zero area intercept indicates the  $R_{\text{ACT}}$  for a large surface area to edge ratio electrode without a heat shield, since all electrode groups have the same edge length to area ratio.

There are several sources of evidence that enhanced transport in TiN electrodes is due to an ionic conducting, electroactive phase within the electrode. TiN generally exhibits enhanced transport without strong temperature activation, and with good transport retained at  $T$  as low as 900K. Some variation is observed in transport enhancement with electrode composition, even though all electrodes contain TiN.

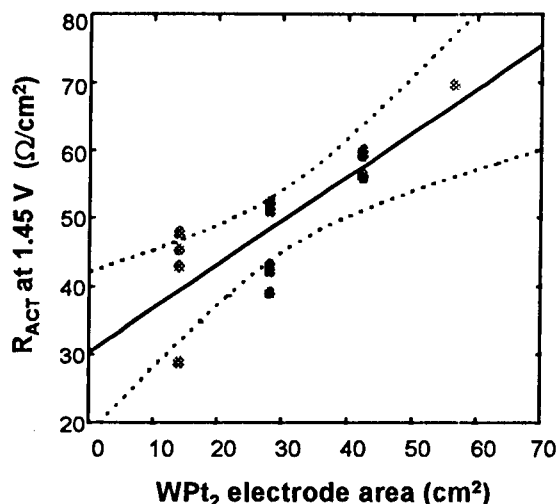


Figure 3:  $R_{\text{ACT}}$  for single  $14.1 \text{ cm}^2$  and combinations of 2, 3, and 4 electrodes operated simultaneously.

TiN electrodes have not generally shown clear activated performance in ETC or SETC tests. All of the TiN electrodes which we have examined are too efficient to be purely free molecular flow electrodes, although they are always somewhat porous by SEM.

Fresh TiN electrodes occasionally show exceptionally good performance. In one SETC test the morphology/transport parameter  $G$  for four electrodes on initial cell warm-up from 880K to 1150 K showed  $G$ 's from 25 to 70 with no significant temperature dependence. Another test showed little variation in limiting currents on initial warm-up from 973K to 1273K. Other TiN electrodes in an SETC showed an apparent small temperature dependence of transport, on cycling from 1123K to 873K and back, after about 600 hours operation in low pressure sodium vapor at 1123K.

Both some fresh TiN electrodes and electrodes modified by small air leaks into the SETC have shown peaks in the current voltage curves before the limiting current is reached, suggesting insertion of  $\text{Na}^+$  and  $e^-$  into a phase within the electrode. These peaks have finite capacity in cyclic voltammogram which implies an electrochemically active phase. A current-voltage curve for a fresh TiN electrode pair at 1223K is shown in Figure 4.

Similar, but exaggerated, peaks are seen in cyclic voltammograms following small air leaks into SETC experiments and these peaks persist for many hours at 1223K in sodium vapor at less than 10 Pa.

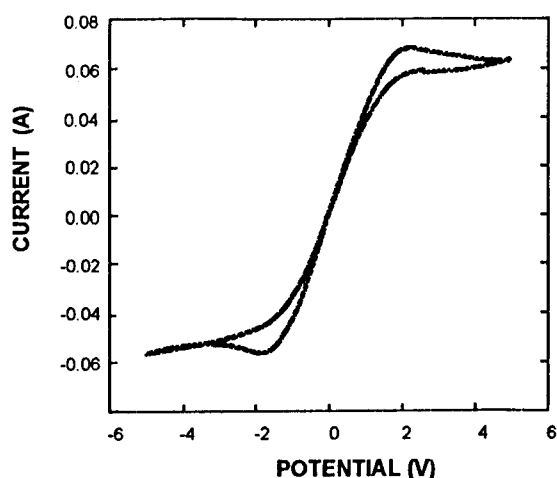


Figure 4: Cyclic voltammogram from SETC of  $\text{Na}_g/\text{TiN}/\text{BASE}/\text{TiN}/\text{Na}_g$  electrochemical cell.

Facile insertion of  $\text{Na}^+$  into an electroactive phase in the TiN electrode suggests the possibility of efficient  $\text{Na}^+$  ionic transport. These peaks are similar to those found in  $\text{Na}_2\text{MoO}_4/\text{Mo}$  electrodes at lower temperatures, on the order of 700-1000K.<sup>10</sup> They persist for many hours in TiN electrodes, even at 1223K, at sodium pressures less than several Pa.

Low frequency arcs in impedance spectra with small associated resistance imply very large associated capacitance or pseudocapacitance. These arcs can be explained as resulting from a pseudocapacitance associated with sodium uptake/loss by the electroactive phase and a resistance change of the ionic conducting phase as its composition changes. At higher frequencies, the composition of this phase will only change very close to the three phase interphase region. However, at low frequencies, a sodium pressure gradient through the whole electrode thickness develops, and the composition and conductivity of the ion conducting phase may change in response to the gradient.

## CONCLUSIONS

Four modes of sodium transport through cathodes in AMTEC cells have been observed, and few electrodes exhibit only one transport mode. The cathode must have efficient sodium transport, an efficient electrochemical charge transfer step, and, with the current collector, low electronic resistance between lead and the charge transfer reaction zone.

Multi-phase electrodes may meet these

requirements with separate phases and therefore be efficient and useful in AMTEC systems. The Faradaic potential of the AMTEC cell is directly affected by the sodium pressure in the charge transfer region through a Nernstian contribution to the potential. The charge transfer region does not distinguish between sodium pressure drops in the exterior of the electrode, or between the electrode exterior and the condenser, as shown experimentally in this paper.

In the cases of some fresh TiN electrodes and some  $\text{WPt}_2$  electrodes the value of  $G$  derived from EIS, is small and varies little with temperature, but the physical morphology of these electrodes indicate that the sodium transport process cannot be very efficient free molecular flow. We conclude that in the case of  $\text{WPt}_2$  a surface or grain boundary sodium diffusion exists in parallel with free molecular flow, partly by analogy with  $\text{WRh}_3$ . The activation energy for some surface or grain boundary diffusion processes may be lower in the case of  $\text{WPt}_2$ , and the parallel free molecular flow diffusion may bypass high activation steps. In the case of TiN, there is electrochemical evidence for an electroactive, ionic conducting phase in the electrode, and its presence explains the efficient transport in these electrodes.

## ACKNOWLEDGEMENTS

The research described in this paper was performed by the Jet Propulsion Laboratory, California Institute of Technology, and was supported by the National Aeronautics and Space Administration.

## REFERENCES

1. N. Weber, "A Thermoelectric Device Based on Beta-Alumina Solid Electrolyte", *Energy Conversion*, **14**, 1-8 (1974).
2. R. M. Williams, M. E. Loveland, B. Jeffries-Nakamura, M. L. Underwood, C. P. Bankston, H. Leduc, and J. T. Kummer, "Kinetics and Transport At AMTEC Electrodes, I.," *J. Electrochem. Soc.*, **137**, 1709-1716 (1990).
3. R. Williams, B. Jeffries-Nakamura, M. Underwood, C. Bankston, and J. Kummer, "Kinetics and Transport At AMTEC Electrodes. II.," *J. Electrochem. Soc.*, **137**, 1716-1723 (1990).
4. R. Williams, B. Wheeler, B. Jeffries-Nakamura, M. Loveland, C. Bankston, and T. Cole, "Effects of

$\text{Na}_2\text{MoO}_4$  and  $\text{Na}_2\text{WO}_4$  on Molybdenum and Tungsten Electrodes for the Alkali Metal Thermoelectric Converter," *J. Electrochem. Soc.*, **135**, 2738 (1988).

5. R. Williams, B. Jeffries-Nakamura, M. Underwood, B. Wheeler, M. Loveland, S. Kikkert, J. Lamb, T. Cole, J. Kummer, and C. Bankston, "High Power Density Performance of WPt and WRh Electrodes in the Alkali Metal Thermoelectric Converter," *J. Electrochem. Soc.*, **136**, 893-894, (1989).

6. B. Wheeler, R. Williams, B. Jeffries-Nakamura, J. Lamb, M. Loveland, C. Bankston, and T. Cole, "Performance and Impedance Studies of Thin, Porous Molybdenum and Tungsten Electrodes for the Alkali Metal Thermoelectric Converter," *J. App. Electrochem.*, **18**, 410 (1988).

7. M. A. Ryan, B. Jeffries-Nakamura, R. M. Williams, M. L. Underwood, D. O'Connor, and S. Kikkert, "Directly Deposited Current Collecting Grids for AMTEC Electrodes", *J. Electrochem. Soc.*, **142**, 4252 (1995).

8. J.R. McBride, D.J. Schmatz, T.K. Hunt and R.F. Novak, "Electrode Materials Research for the Sodium Heat Engine", *Proc. Second Symp. on Electrode Mat. and Processes for Energy Conversion and Storage*, Electrochemical Society, Vol. 87-12, p. 594 (1987).

9. Q. Fang and H. Wendt, "Performance and Thermodynamic Properties of Na-Sn and Na-Pb Molten Alloy Electrodes for Alkali-Metal Thermoelectric Converter", *J. App. Electrochem.*, **26**, 343-352 (1996).

10. R. M. Williams, C. Bankston, C. P., Khanna, S. K., and Cole, T., "Voltammetric Studies of Porous Molybdenum Electrodes for the Alkali Metal Thermoelectric Converter," *J. Electrochem. Soc.*, **133**, 2253 (1986).

11. R. Williams, G. Nagasubramanian, S. Khanna, C. Bankston, A. Thakoor, and T. Cole, "The Role of Oxygen in Porous Molybdenum Electrodes for the Alkali Metal Thermoelectric Converter," *J. Electrochem. Soc.*, **133**, 1587 (1986).

12. T.K. Hunt, D.J. Schmatz, J.R. McBride, R.F. Novak and M.A. Dzieciuch, "Solid State Electrode Systems for the Sodium Heat Engine", *Proc. Second Symp. on Electrode Mat. and Processes for Energy Conversion and Storage*, Electrochemical Society, Vol 87-12, p. 608 (1987).

13. H. Nakata, T. Nagata, K. Tsuchida, and A. Kato,

"Ceramic Electrodes for an Alkali-Metal Thermoelectric Converter (AMTEC), *J. App. Electrochem.*, **23**, 1251-1258, (1993).

14. Q. Fang and R. Knodler "Porous TiB<sub>2</sub> Electrodes for the Alkali-Metal Thermoelectric Converter ", *J. Mat. Sci.*, **27**, 6725-6729 (1992).

15. O. Asakami, K. Tsuchida, H. Tagawa, and A. Kato. "Material for the Electrode of the Alkali-Metal Thermoelectric Converter, (AMTEC), *J. Mat. Sci Lett.* , **8**, 1141-1143, (1989)

16. T. Hashimoto, K. Shibata, K. Tsuchida, and A. Kato, "Screen-printed Electrode for Alkali-Metal Thermoelectric Converter", *J. Mat. Sci Lett.*, **11**, 745-748, (1992).

17. O. Asakami, K. Tsuchida, A. Kato "Material for the Electrode of the Alkali-Metal Thermoelectric Converter, (AMTEC) (II)", *J. Mat. Sci Lett.*, **9**, 892-894, (1990).

18. E. H. Kennard, "Kinetic Theory of Gases", p69 McGraw-Hill Book Co., New York (1938).